Biointerface Research in Applied Chemistry
Open-Access Journal (ISSN: 2069-5837)

Article
Volume 13, Issue 4., 2023, 392
https://doi.org/10.33263/BRIAC134.392

Drug Delivery Assessments of Hydroxyurea Anticancer by an Epoxy-Decorated Fullerene Cage

Kun Harismah[1,*], Ali Hassan[2], Omar Talal Hamid[3], Mohammed A. Saadoon[4], Hasan Zandi [5]

[1] Department of Chemical Engineering, Faculty of Engineering, Universitas Muhammadiyah Surakarta, Surakarta, Indonesia; kun.harismah@ums.ac.id (K.H.);
[2] Department of Medical Instrumentation Engineering Techniques, Bilad Alrafidain University College, Diyala, Iraq; alihabeel@hotmail.com (A.H.);
[3] Department of Oil and Gas Refining Engineering, Al-Turath University College, Baghdad, Iraq; omar.talal@turath.edu.iq (O.T.H.);
[4] Directorate General of Education Karkh 1, Ministry of Education, Baghdad, Iraq; mohammedsadoon16@gmail.com (M.A.S.);
[5] Department of Chemistry, Faculty of Science, University of Qom, Qom, Iran; h.zandi.dr@gmail.com (H.Z.);
* Correspondence: kun.harismah@ums.ac.id (K.H.);

Scopus Author ID 56982926300
Received: 23.06.2022; Accepted: 18.07.2022; Published: 1.11.2022

Abstract: By the importance of innovating novel protocols of drug delivery processes, an idea of employing an epoxy-decorated fullerene cage (OFC) for the drug delivery of hydroxyurea (HU) anticancer was assessed in this work by performing density functional theory (DFT) molecular computations. Singular models of HU and OFC were optimized to be prepared for participating in the interaction processes for evaluating the adsorption features. The results yielded different HU@OFC bimolecular models based on different configurations of HU towards the epoxy-decorated active site of OFC. Interactions, details, and strengths affirmed the formation of such bimolecular models. Three types of H…O, O…C, and O…O interactions were observed in the formation of bimolecular models, in which H…O and O…C showed the highest importance for formations of the HU@OFC bimolecular models with the highest strengths. Additionally, the molecular orbitals features showed the benefits of these models for approaching diagnostic purposes and structural/electronic specifications. The evaluated features indicated variations of frontier molecular orbitals among the models besides the occurrence of variations for other levels. Consequently, the models of HU@OFC were found to be suitable for employment in the drug delivery processes regarding the specified structural and electronic requirements.

Keywords: anticancer; hydroxyurea; fullerene; adsorption; DFT

1. Introduction

Since the early innovation of carbon nanotubes (CNTs), attention has been paid to the recognition of features of such novel materials [1-3]. Pure carbon composition and other non-carbon compositions have been proposed to develop the borders of nanostructures applications [4-6]. Among such investigations, modifying nanostructures with other atomic and molecular groups has been seen as useful for specifying the applications of newly decorated nanostructures [7-9]. In this regard, oxidation has been seen as important for modifying carbon-based nanostructures to improve their physical and chemical features [10-12]. To this aim, the

functionalization of nanostructures by an epoxy group could yield to the successful production of oxidized carbon nanostructures [13-15]. The newly decorated nanostructure region could indeed work as an active site of interactions with other substances, especially for those with the potential to contribute to hydrogen bond interactions [16]. It was also assumed that the oxidized carbon nanostructures could be dispersed in water media better than the pure carbon nanostructures [17]. Hence, the idea of employing oxidized carbon nanostructures for interacting with other heteroatomic substances could be supported. The wide surface area has always been a remarkable advantage of interacting substances and adsorbents, in which the decorated models of nanostructures could provide activated surfaces for participating in the efficient adsorption processes [18-20].

In the current research work, a model of an epoxy-decorated fullerene cage (OFC) was investigated for the drug delivery assessments of hydroxyurea (HU) anticancer (Figure 1). A suitable model of carbon-20 for molecular investigations was decorated by an epoxy group to yield the oxidized fullerene cage. Next, possible interactions between HU and OFC were investigated to examine the existence of HU@OFC bimolecular complexes (Figure 2). In this regard, structural optimization calculations and electronic feature evaluations were done to approach the required results of this work. Earlier works indicated that the nanostructures could work in the drug delivery processes and that innovating novel carriers could help with this [21-23]. Several efforts have been made to explore the benefits of nanostructures and their modified models to work as carriers of drug substances to this time [24]. Indeed, the phenomena of drug design and development is a non-stop process, and improvements are always required [25-29]. Accordingly, performing molecular computations could provide information on details of such drug-related processes [30-33]. For the case of anticancer, investigating new drug delivery protocols is essential because of the low efficacy of conventional protocols [34-36]. HU is also among the anticancer with the dual edge of advantage/disadvantage of medications for cancer patients [37-39]. To improve the advantages and overcome the disadvantages, exploring novel carriers could help conduct the HU substance through a targeted drug delivery process [40]. To this aim, this work was done for the drug delivery assessments of HU with the assistance of OFC nanostructure. To this aim, this work was done for the drug delivery assessments of HU with the assistance of OFC nanostructure. The obtained results of this work are exhibited in Tables 1 and 2 and Figures 1-3.

2. Materials and Methods

The drug delivery assessment of hydroxyurea (HU) anticancer with the assistance of an epoxy-decorated fullerene cage (OFC) was investigated in this work by means of 3D molecular models and computations. First, singular OFC and HU geometries were optimized to prepare the original models (Figure 1). The structure of OFC was created by an epoxy-decoration of a carbon-20 fullerene cage to yield a model with the $C_{20}O$ formula for adsorbing the HU substance with the $CH_4N_2O_2$ formula. Next, HU@OFC bimolecular models were obtained by re-optimizing the combinations of already optimized OFC and HU models. All possible configurations of HU@OFC complexes were examined by considering all interaction directions between HU and OFC; it should be noted that the epoxy-decorated region of OFC was the active site of interaction with the HU substance. As shown in Figure 2, four HU@OFC models, H1-H4, were finalized, representing the interaction modes of HU and OFC as described by the features of the quantum theory of atoms in molecules (QTAIM) (Table 1). Subsequently, additional features, including energies of adsorption and frontier molecular

orbitals of the models, were evaluated (Table 2). For better representing such molecular orbital features, energy levels of the highest occupied and the lowest unoccupied molecular orbitals (HOMO and LUMO) and the corresponding distribution patterns were evaluated for the models (Table 2 and Figures 1 and 2). Moreover, diagrams of the density of states (DOS) were illustrated for the models (Figure 3) to show the possibility of a diagnosis of HU@OFC bimolecular formations. All results of this work were evaluated by performing B3LYP/6-31G* density functional theory (DFT) molecular computations using the Gaussian program [41]. It should be mentioned that several research methodologies have been developed to investigate chemical and biochemical systems. Both experimental and computational methodologies could be employed for dealing with the targeted problems [42-46]. This work was done using computational tools to describe the complicated model systems at the smallest molecular and atomic scales [47-49].

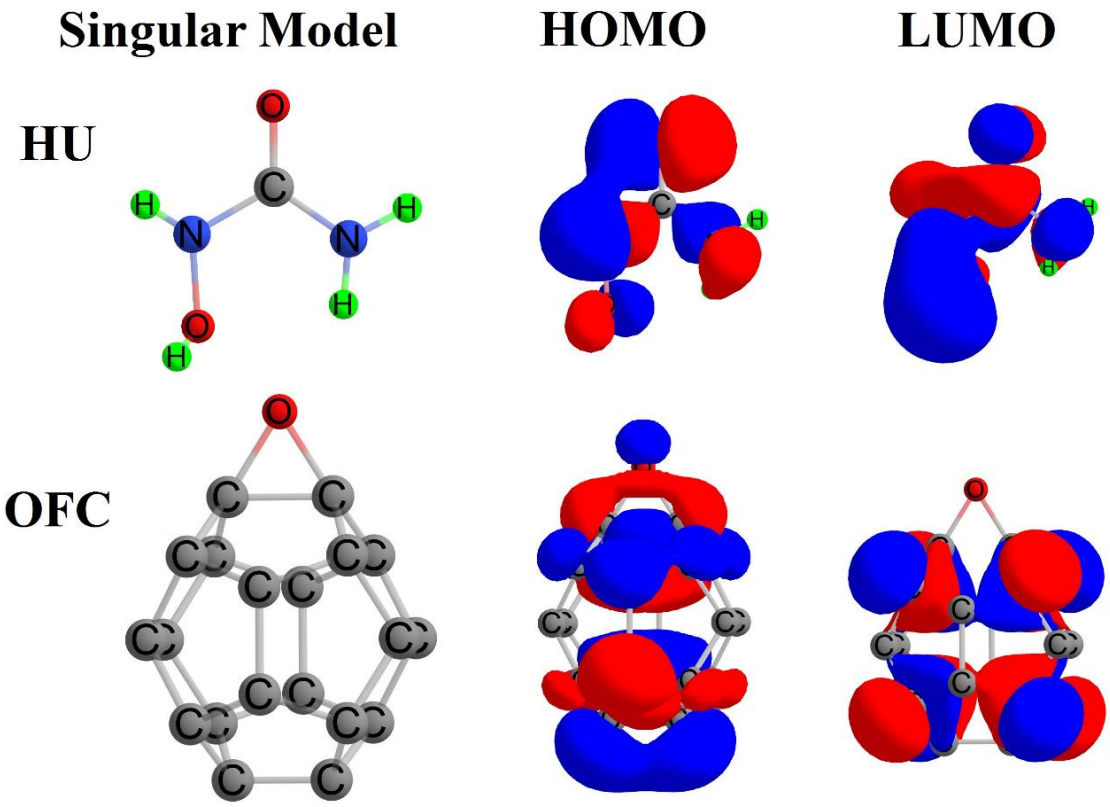

Figure 1. Singular models and HOMO-LUMO distribution patterns.

3. Results and Discussion

This work was done for the drug delivery assessments of hydroxyurea (HU) anticancer by an epoxy-decorated fullerene cage (OFC). To this aim, DFT molecular computations were performed to recognize the stabilized structures of singular HU and OFC, as shown in Figure 1, to prepare them as the original materials for participating in the HU@OFC bimolecular formations. All possible interacting configurations of these two molecules were examined by initiating different starting geometries of the singular models towards each other. Next, the optimized stabilized HU@OFC bimolecular models were found in four different configurations based on the interactions of atomic sites of HU by the epoxy active site of OFC, as shown in Figure 2 by H1, H2, H3, and H4. First, it should be mentioned that both singular and bimolecular models were suitable for formation according to their final geometrical configurations. The models were optimized to reach the minimized energy geometries in this

regard. Subsequently, details of such interacting systems were recognized by performing additional QTAIM analyses [50-52]. As listed in Table 1, the bimolecular models were described by types of interactions, distances, total electron density (Rho), Laplacian of electron density (Del^2-Rho), and energy of electron density (H). The models were characterized by the existence of meaningful interactions between HU and OFC substances in each of the HU@OFC bimolecular models. Accordingly, the types of interactions indicated the important role of the epoxy-decorated region in conducting the interaction processes. The oxygen atom of OFC and the neighboring carbon atom were important for contributing to interactions with the HU substance through formations of O…C interactions. In the investigated models, physical interactions were observed to provide an environment of reversible adsorption for the drug delivery process.

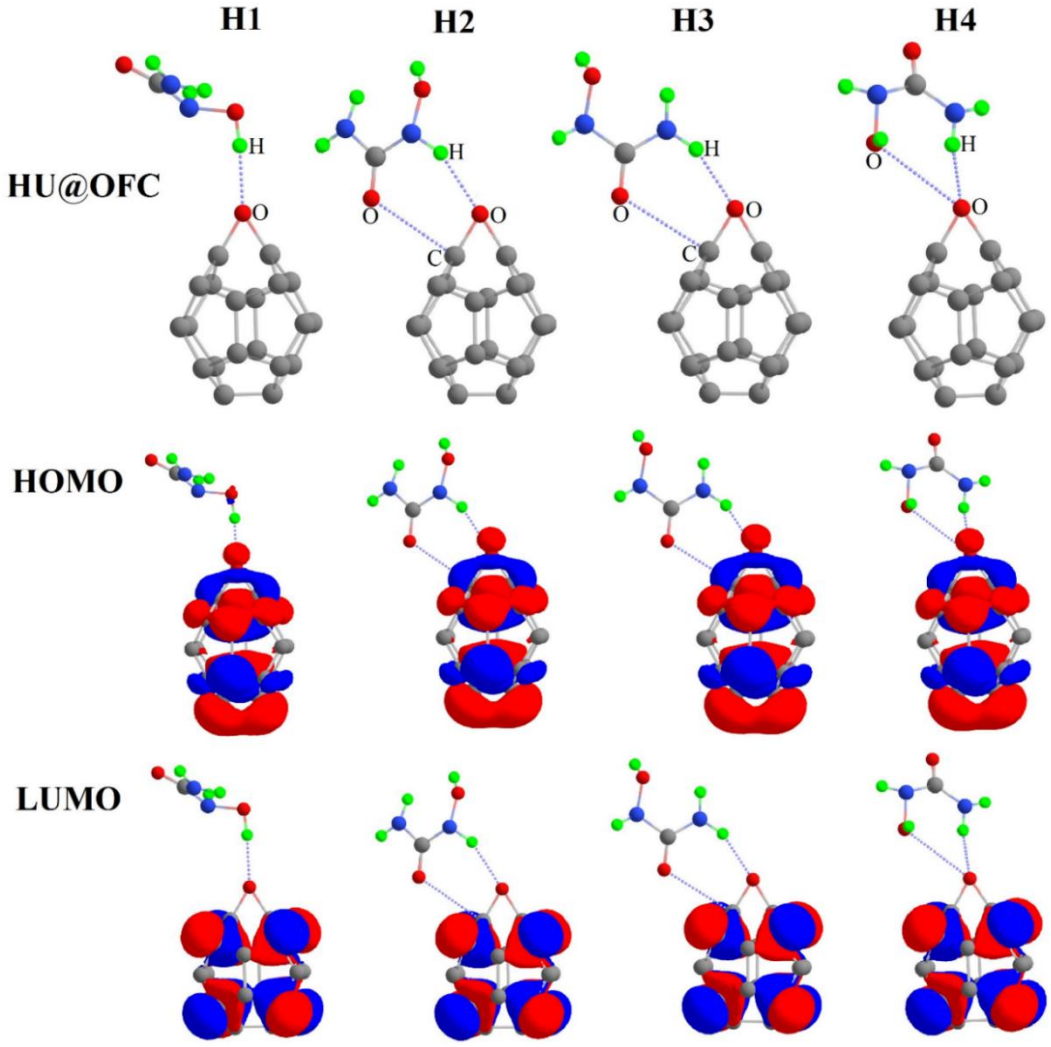

Figure 2. Bimolecular models and HOMO-LUMO distribution patterns.

Table 1. The evaluated QTAIM features of HU@OFC models.[1]

HU@OFC Model	HU…OFC Interaction	Distance	Rho × 100	Del^2-Rho × 100	H × 100
H1	H…O	1.95	12.33	7.89	-1.97
H2	H…O O…C	2.11 2.98	16.68 8.69	5.84 3.08	-4.59 -1.08
H3	H…O O…C	2.11 2.98	16.53 8.69	5.85 3.08	-4.32 -1.08
H4	H…O O…O	2.19 3.06	14.61 6.57	4.89 2.53	-1.64 -0.56

[1]The units: Distance: Å; Rho, Del^2-Rho, and H: au.

Based on obtained results of Table 1 for the interacting HU@OFC bimolecular models of Figure 2, different strengths of interactions were found for the observed types of interactions, including H…O, O…O, and O…C in the stabilized H1-H4 models. The observed strength was found to be different from the evaluated QTAIM features, but they were still meaningful for the formations of bimolecular models. In this regard, the types of involving interactions indicated the final configurations of HU@OFC complexes by considering all possible interacting configurations. In this step, it was found that the models were in different configurations of interactions for obtaining the models of HU@OFC bimolecular complexes.

Table 2. The evaluated energy features of singular and bimolecular models.[1]

Model	E_{Ads}	HOMO	LUMO	E_{Gap}	E_{Fermi}
HU	n/a	-6.96	0.96	7.93	-3.00
OFC	n/a	-5.41	-3.32	2.10	-4.37
H1	-47.17	-5.70	-3.59	2.11	-4.64
H2	-48.27	-5.24	-3.13	2.11	-4.19
H3	-48.22	-5.25	-3.13	2.12	-4.19
H4	-40.56	-5.67	-3.57	2.10	-4.62

[1]The units: E_{Ads}: kcal/mol; HOMO, LUMO, E_{Gap}, and E_{Fermi}: eV.

The main idea of this work was to develop a new carrier for the drug delivery of HU, and the proposed OFC model was assessed to approach the idea. As exhibited in Figure 2, the formations of HU@OFC bimolecular models were achievable, and details of interactions were recognized by the evaluated QTAIM feature of Table 1. Subsequently, the energy features of the investigated models are summarized in Table 2. By comparing the adsorption energy values (E_{Ads}), it was found that the bimolecular models were in different levels of strength based on the obtained values of E_{Ads}. The order of H2 > H3 > H1 > H4 was extracted for the bimolecular models to show their adsorption strength. As mentioned earlier, for the evaluated QTAIM features, different types of interactions were available for the bimolecular models with more or less meaningful strength in compassion with each other. Accordingly, the observed values of E_{Ads} showed different levels of strength for the adsorption process of HU anticancer towards the OFC active site. In this regard, H2 and H3 with similar types of interactions but different configurations were placed at the highest level of adsorption strength by the obtained E_{Ads} values of -48.27 and -48.22 kcal/mol, respectively. H1 and H4 were placed at the next levels of strength by the obtained E_{Ads} values of -47.17 and -40.56 kcal/mol, respectively. The H…O and O…C interactions between HU and OFC of H2 and H3 were dominant for the formation of stronger adsorbing systems, whereas only one H…O interaction of H1 and H…O and O…O interactions of H4 were not so strong as those of H2 and H3. It should be mentioned that all four HU@OFC models were strong enough to consider the characteristic role of OFC for adsorbing the HU substance. Comparing the results of this work with those of an earlier work [40] could show the benefits of employing the current system for conducting the drug delivery process of HU anticancer. The model of functionalized nanostructure could even work better than the pure nanostructure to provide an active site of interaction with the drug substance. Indeed, such a decorated surface could make a more efficient adsorption process possible for forming bimolecular HU@OFC complexes.

Further assessments of the models were done by analyzing the HOMO-LUMO distribution patterns, in which all bimolecular models showed a movement of such patterns to the OFC part. This is indeed a very important point for the drug delivery processes, in which the models should have the role of drug protection, avoiding their contribution to unwanted interactions. In this regard, the models of HU@OFC bimolecular complexes showed such features by movements of all HOMO-LUMO patterns to the OFC part. Another achievement

was the HOMO-LUMO shapes of bimolecular models, which were closer to the singular OFC model. Accordingly, the obtained values of energy levels of HOMO and LUMO of bimolecular models were closer to the singular OFC model. This achievement was important because OFC's diagnostic role for the adsorption of HU, as the energy distances of HOMO-LUMO levels (E_{Gap}) were found in different values. Not only for the values of E_{Gap}, but also different values of energy of Fermi level (E_{Fermi}) were different in the bimolecular models with a closer value to the singular OFC model. As a result, the illustrated diagrams of DOS (Figure 3) exhibited variations of an electronic system for approaching the diagnostic features as shown by the DOS diagrams, molecular orbital features of before and after HOMO and LUMO levels detected variations in the occurrence of adsorption processes with different configurations. In this regard, the models were found to be balanced for a specified application based on the required electronic and structural requirements. Consequently, the assessments of this work showed the successful role of OFC in working in the drug delivery of HU anticancer.

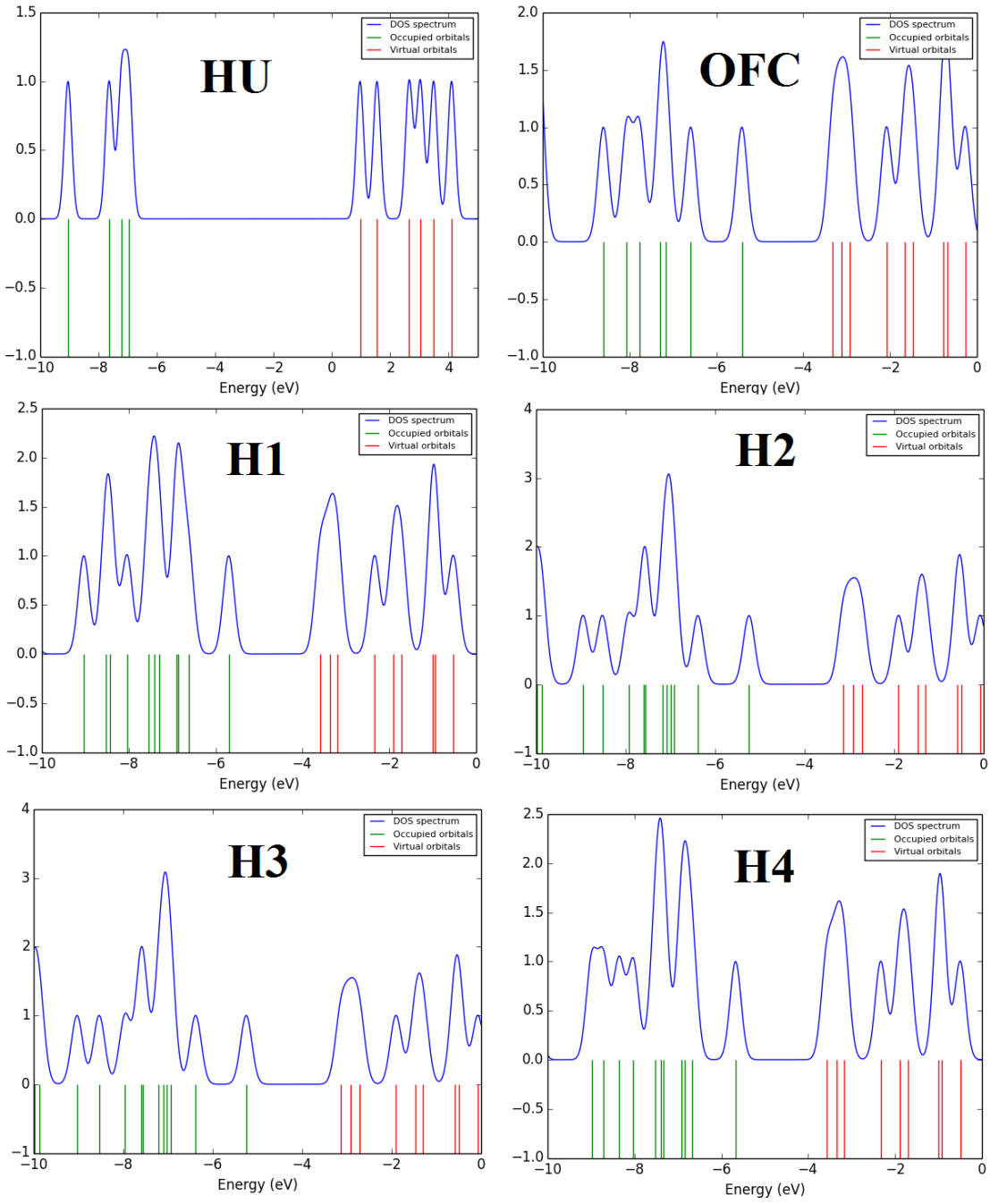

Figure 3. DOS diagrams of singular and bimolecular models.

4. Conclusions

Drug delivery assessments of hydroxyurea (HU) anticancer by an epoxy-decorated fullerene cage (OFC) were done in this work by employing DFT molecular computations of singular and bimolecular models. To approach the goal of this work, all possible interacting configurations of HU and OFC were examined, in which the results yielded four HU@OFC bimolecular models; H1, H2, H3, and H4, involving H…O, O…O, and O…C interactions between two substances. In this regard, details of interactions and strengths affirmed the formation of HU@OFC bimolecular models. Further analyses of the models were done by the evaluated molecular orbitals features, in which HOMO-LUMO distribution patterns and DOS diagrams showed variations of such molecular orbitals in the bimolecular models close to the variations of singular OFC. This achievement was advantageous for approaching the diagnostic purposes of HU@OFC bimolecular formations besides balancing the structural and electronic features for specified purposes. As a final remark, the assessments of this work successfully showed the dominant role of OFC in the drug delivery of HU anticancer.

Funding

This research received no external funding.

Acknowledgments

This research has no acknowledgment.

Conflicts of Interest

The authors declare no conflict of interest.

References

1. Jasem, N.; Al-Quzweny, M.; Alsammarraie, A. Spectroscopic investigation of carbon nanostructures. *Chemical Methodologies* **2022,** *6,* 237–245, https://doi.org/10.22034/chemm.2022.322390.1416.
2. Afzal, F.; Afzal, F.; Afzal, D.; Farahani, M.; Hussain, Z.; Cancan, M. Weighted entropies of HAC5C7[p;q] nanotube. *Eurasian Chemical Communications* **2021,** *3,* 1–5, https://doi.org/10.22034/ecc.2021.119835.
3. Afzal, F.; Cancan, M.; Ediz, S.; Afzal, D.; Chaudhry, F.; Farahani, M. Degree-based entropy of molecular of HAC5C7[P,Q]. *Eurasian Chemical Communications* **2021,** *3,* 291–295, https://doi.org/10.22034/ecc.2021.278787.1156.
4. Farhadi, B.; Ebrahimi, M.; Morsali, A. Microextraction and determination trace amount of propranolol in aqueous and pharmaceutical samples with oxidized multiwalled carbon nanotubes. *Chemical Methodologies* **2021,** *5,* 227–233, https://doi.org/10.22034/chemm.2021.125471.
5. Shamsi, A.; Ahour, F. Electrochemical sensing of thioridazine in human serum samples using modified glassy carbon electrode. *Advanced Journal of Chemistry-Section A* **2021,** *4,* 22–31, https://doi.org/10.22034/ajca.2020.252025.1215.
6. Hassani, M.; Zeeb, M.; Monzavi, A.; Khodadadi, Z.; Kalaee, M. Response surface modeling and optimization of microbial fuel cells with surface-modified graphite anode electrode by ZSM-5 nanocatalyst functionalized. *Chemical Methodologies* **2022,** *6,* 253–268, https://doi.org/10.22034/chemm.2022.324312.1425.
7. Ahmed, H.; Abdulrahman, N. Effect of magnetic field on the preparation of Cu doped zinc oxide nanostructures in different temperatures. *Eurasian Chemical Communications* **2021,** *3,* 443–451, https://doi.org/10.22034/ecc.2021.282390.1171.
8. Ali, M.; Islam, M.; Rafid, M.; Ahmed, R.; Jeetu, M.; Roy, R.; Chakma, U.; Kumer, A. The computational screening of structural, electronic, and optical properties for SiC, Si0.94Sn0.06C, and Si0.88Sn0.12C lead-free photovoltaic inverters using DFT functional of first principle approach. *Eurasian Chemical Communications* **2021,** *3,* 327–338, https://doi.org/10.22034/ecc.2021.278690.1154.

9. Darougari, H.; Rezaei-Sameti, M. The drug delivery appraisal of Cu and Ni decorated B12N12 nanocage for an 8-hydroxyquinoline drug: a DFT and TD-DFT computational study. *Asian Journal of Nanosciences and Materials* **2022,** *5*, 196–210, https://doi.org/10.26655/AJNANOMAT.2022.3.3.
10. Hamidi Zare, S.; Ghorayshi Nejad, M.S.; Saberi, A.; Rostami, E. A highly efficient and sustainable synthesis of 1-[(1,3-thiazol-2-ylamino) methyl]-2-naphthols under solvent-free conditions using graphene oxide substituted ethane sulfonic acid catalyst. *Asian Journal of Nanosciences and Materials* **2022,** *5*, 211–224, https://doi.org/10.26655/AJNANOMAT.2022.3.4.
11. Kreydie, S.; Al-Abdaly, B. Synthesis, characterization and evaluation of inhibition corrosion of bacterial cellulose/metal oxides nanocomposites. *Eurasian Chemical Communications* **2021,** *3*, 706–714, https://doi.org/10.22034/ecc.2021.299439.1216.
12. Muhi-Alden, Y.; Saleh, K. Removing methylene blue dye from industrial wastewater using polyacrylonitrile/iron oxide nanocomposite. *Eurasian Chemical Communications* **2021,** *3*, 755–762, https://doi.org/10.22034/ecc.2021.300767.1225.
13. Elhenawy, Y.; Fouad, Y.; Marouani, H.; Bassyouni, M. Performance analysis of reinforced epoxy functionalized carbon nanotubes composites for vertical axis wind turbine blade. *Polymers* **2021,** *13*, 422, https://doi.org/10.3390/polym13030422.
14. Begum, S.; Ullah, H.; Ahmed, I.; Zhan, Y.; Kausar, A.; Aleem, M.A.; Ahmad, S. Investigation of morphology, crystallinity, thermal stability, piezoelectricity and conductivity of PVDF nanocomposites reinforced with epoxy functionalized MWCNTs. *Composites Science and Technology* **2021,** *211*, 108841, https://doi.org/10.1016/j.compscitech.2021.108841.
15. Yasaroglu, I.; Aras, O.; Kaya, Y. Qualitative study on the effects of hydroxyl functionalized multiwall carbon nanotube and silica doped-epoxy composites. *Polymer Composites* **2022,** *43*, 1462–1475, https://doi.org/10.1002/pc.26466.
16. Mirzaei, M.; Gulseren, O.; Rafienia, M.; Zare, A. Nanocarbon-assisted biosensor for diagnosis of exhaled biomarkers of lung cancer: DFT approach. *Eurasian Chemical Communications* **2021,** *3*, 154–161, https://doi.org/10.22034/ecc.2021.269256.1126.
17. Lavagna, L.; Nisticò, R.; Musso, S.; Pavese, M. Functionalization as a way to enhance dispersion of carbon nanotubes in matrices: a review. *Materials Today Chemistry* **2021,** *20*, 100477, https://doi.org/10.1016/j.mtchem.2021.100477.
18. Hanafizadeh, P.; Karimi, A.; Taklifi, A.; Hojati, A. Experimental investigation of two-phase water–oil flow pressure drop in inclined pipes. *Experimental Thermal and Fluid Science* **2016,** *74*, 169–180, https://doi.org/10.1016/j.expthermflusci.2015.11.024.
19. Dehno Khalaji, A.; Machek, P.; Jarosova, M. α-Fe2O3 nanoparticles: synthesis, characterization, magnetic properties and photocatalytic degradation of methyl orange. *Advanced Journal of Chemistry-Section A* **2021,** *4*, 317–326, https://doi.org/10.22034/ajca.2021.292396.1268.
20. Rostamzadeh Mansour, S.; Sohrabi-Gilani, N.; Nejati, P. Synthesis and characterization of a nanomagnetic adsorbent modified with thiol for magnetic and investigation of its adsorption behavior for effective elimination of heavy metal ions. *Advanced Journal of Chemistry-Section A* **2022,** *5*, 31–44, https://doi.org/10.22034/ajca.2022.308695.1283.
21. Pari, A.A.; Yousefi, M.; Samadi, S.; Allahgholi Ghasri, M.R.; Torbati, M.B. Structural analysis of an iron-assisted carbon monolayer for delivery of 2-thiouracil. *Main Group Chemistry* **2021,** *20*, 653–661, https://doi.org/10.3233/mgc-210079.
22. Hatami, A.; Heydarinasab, A.; Akbarzadehkhiyavi, A.; Pajoum Shariati, F. An introduction to nanotechnology and drug delivery. *Chemical Methodologies* **2021,** *5*, 153–165, https://doi.org/10.22034/chemm.2021.121496.
23. Hosseini, S.A.; Shojaie, F.; Afzali, D. Analysis of structural, and electronic properties of clopidogrel drug adsorption on armchair (5, 5) Single-walled carbon nanotube. *Asian Journal of Nanosciences and Materials* **2021,** *4*, 15–30, https://doi.org/10.26655/AJNANOMAT.2021.1.2.
24. Makvandi, P.; Josic, U.; Delfi, M. et al. Drug delivery (nano) platforms for oral and dental applications: tissue regeneration, infection control, and cancer management. *Advanced Science* **2021,** *8*, 2004014, https://doi.org/10.1002/advs.202004014.
25. Makani Bassakouahou, J.; Kouala Landa, C.; Kimbally-Kaky, E.; Bakekolo, P.; Ellenga Mbolla, B.; Ikama, M. Aortic remodeling and human immunodeficiency virus infection: two case reports. *International Journal of Scientific Research in Dental and Medical Sciences* **2021,** *3*, 190–192, https://doi.org/10.30485/ijsrdms.2021.306038.1194.

26. Alfayate, R.P.; Suarez, A.; Algar Pinilla, J. CBCT Management of previously treated mandibular incisor with extensive internal root resorption: a case report. *International Journal of Scientific Research in Dental and Medical Sciences* **2020,** *2*, 141–144, https://doi.org/10.30485/ijsrdms.2020.254227.1095.
27. Solano, N.; Perez, L.; Rivera, E.; Medina, C. Hybrid odontogenic tumor with a unique presentation of the calcifying epithelial odontogenic tumor, adenomatoid odontogenic tumor, and calcifying odontogenic cyst: a case report. *International Journal of Scientific Research in Dental and Medical Sciences* **2021,** *3*, 50–54, https://doi.org/10.30485/ijsrdms.2021.269482.1106.
28. Solano, N.; Castrillo, A.; Parra, E.; Medina, C. A huge orofacial myiasis, the importance of ideal management: a case report. *International Journal of Scientific Research in Dental and Medical Sciences* **2020,** *2*, 17–19, https://doi.org/10.30485/ijsrdms.2020.217841.1036.
29. Sahraian, M.A.; Shahmohammadi, A.; Shahmohammadi, S.; Doosti, R. Leukoencephalopathy with brain stem and spinal cord involvement and lactate elevation (LBSL) based on typical MRI and MRS findings: a case report. *International Journal of Scientific Research in Dental and Medical Sciences* **2022,** *4*, 38–41, http://doi.org/10.30485/ijsrdms.2022.325233.1241.
30. Adole, V. Synthesis, antibacterial, antifungal and DFT studies on structural, electronic and chemical reactivity of (E)-7-((1H-Indol-3-yl)methylene)-1,2,6,7-tetrahydro-8H-indeno[5,4-b]furan-8-one. *Advanced Journal of Chemistry-Section A* **2021,** *4*, 175–187, http://doi.org/10.22034/ajca.2021.278047.1250.
31. Farhami, N. A computational study of thiophene adsorption on boron nitride nanotube. *Journal of Applied Organometallic Chemistry* **2022,** *2*, 163–172, http://doi.org/10.22034/jaoc.2022.154821.
32. Oyeneyin, O.; Abayomi, T.; Ipinloju, N.; Agbaffa, E.; Akerele, D.; Arobadade, O. Investigation of amino chalcone derivatives as anti-proliferative agents against MCF-7 breast cancer cell lines-DFT, molecular docking and pharmacokinetics studies. *Advanced Journal of Chemistry-Section A* **2021,** *4*, 288–299, https://doi.org/10.22034/ajca.2021.285869.1261.
33. Venkatesh, G.; Sheena Mary, Y.; Shymamary, Y.; Palanisamy, V.; Govindaraju, M. Quantum chemical and molecular docking studies of some phenothiazine derivatives. *Journal of Applied Organometallic Chemistry* **2021,** *1*, 148–158, https://doi.org/10.22034/jaoc.2021.303059.1033.
34. Mezoughi, A.; Abdussalam-Mohammed, W.; Abdusalam, A. Synthesis and molecular docking studies of some thiohydantoin derivatives as potential anticancer and antimicrobial agents. *Advanced Journal of Chemistry-Section A* **2021,** *4*, 327–338, https://doi.org/10.22034/ajca.2021.291823.1266.
35. Oladipupo, A.; Alaribe, C.; Akintemi, T.; Coker, H. Effect of phaulopsis falcisepala (acanthaceae) leaves and stems on mitotic arrest and induction of chromosomal changes in meristematic cells of allium cepa. *Progress in Chemical and Biochemical Research* **2021,** *4*, 134–147, https://doi.org/10.22034/pcbr.2021.256993.1163.
36. Hatami, A.; Azizi Haghighat, Z. Evaluation of application of drug modeling in treatment of liver and intestinal Cancer. *Progress in Chemical and Biochemical Research* **2021,** *4*, 220–233, https://doi.org/10.22034/pcbr.2021.277514.1181.
37. Musiałek, M.W.; Rybaczek, D. Hydroxyurea—the good, the bad and the ugly. *Genes* **2021,** *12*, 1096, https://doi.org/10.3390/genes12071096.
38. Heitzer, A.M.; Longoria, J.; Okhomina, V.; Wang, W.C.; Raches, D.; Potter, B.; Jacola, L.M.; Porter, J.; Schreiber, J.E.; King, A.A.; Kang, G.; Hankins, J.S. Hydroxyurea treatment and neurocognitive functioning in sickle cell disease from school age to young adulthood. *British Journal of Haematology* **2021,** *195*, 256–266, https://doi.org/10.1111/bjh.17687.
39. Kapor, S.; Čokić, V.; Santibanez, J.F. Mechanisms of hydroxyurea-induced cellular senescence: an oxidative stress connection? *Oxidative Medicine and Cellular Longevity* **2021,** *2021*, 7753857, https://doi.org/10.1155/2021/7753857.
40. Li, W.; Zhao, T. Hydroxyurea anticancer drug adsorption on the pristine and doped C70 fullerene as potential carriers for drug delivery. *Journal of Molecular Liquids* **2021,** *340*, 117226, https://doi.org/10.1016/j.molliq.2021.117226.
41. Frisch, M.J.; Trucks, G.W.; Schlegel, H.B. et al. *Gaussian 09 program*. Gaussian Inc. Wallingford, CT, **2009**.
42. Mohajer, F.; Mohammadi Ziarani, G.; Badiei, A. New advances on Modulating nanomagnetic cores as the MRI-monitored drug release in cancer. *Journal of Applied Organometallic Chemistry* **2021,** *1*, 143–147, https://doi.org/10.22034/jaoc.2021.301405.1032.
43. Da'i, M.; Suhendi, A.; Meiyanto, E.; Jenie, U.A.; Kawaichi, M. Apoptosis induction effect of curcumin and its analogs pentagamavunon-0 and pentagamavunon-1 on cancer cell lines. *Asian Journal of Pharmaceutical and Clinical Research* **2017,** *10*, 373–376, https://doi.org/10.22159/ajpcr.2017.v10i3.16311.

44. Jamali, S.; Ahmadi, F.; Mahdavi-Mazdeh, M.; Tavoosi, A. The relationship between serum uric acid level and pulmonary artery hypertension in patients with chronic renal failure. *International Journal of Scientific Research in Dental and Medical Sciences* **2019,** *1,* 23–25, https://doi.org/10.30485/ijsrdms.2019.89759.
45. Wikantyasning, E.R.; Mutmainnah, M.; Cholisoh, Z.; Hairunisa, I.; Bakar, M.F.A.; Da'i, M. Preparation of hydrogel nanocomposite containing gold nanoparticles with unique swelling/deswelling properties. *Rasayan Journal of Chemistry* **2019,** *12,* 1857–1863, https://doi.org/10.31788/rjc.2019.1245209.
46. Seyedashrafi, M.M.; Jamali, J.; Rezaie, A.; Jamali, A.H. Identify the dentistry students perception of the learning environment (LE): a literature review. *International Journal of Scientific Research in Dental and Medical Sciences* **2020,** *2,* 12–16, https://doi.org/10.30485/ijsrdms.2020.217432.1035.
47. Ghiasifar, M.; Hosseinnejad, T.; Ahangar, A. Copper catalyzed cycloaddition reaction of azidomethyl benzene with 2,2-di(prop-2-yn-1-yl)propane-1,3-diol: DFT and QTAIM investigation. *Progress in Chemical and Biochemical Research* **2022,** *5,* 1–20, https://doi.org/10.22034/pcbr.2022.319090.1203.
48. Mirzaei, M.; Rasouli, A.H.; Saedi, A. HOMO-LUMO photosensitization analyses of coronene-cytosine complexes. *Main Group Chemistry* **2021,** *20,* 565–573, https://doi.org/10.3233/mgc-210078.
49. Basafa, S.; Davoodnia, A.; Beyramabadi, S.; Pordel, M. A probe into hydrolysis of nitrile moiety in 2-amino-1-methyl-4-oxo-1,4-dihydroquinoline-3-carbonitrile. *Chemical Methodologies* **2021,** *5,* 59–69, https://doi.org/10.22034/chemm.2021.118891.
50. Wilson, T.R.; Alexandrova, A.N.; Eberhart, M.E. Electron density geometry and the quantum theory of atoms in molecules. *The Journal of Physical Chemistry A* **2021,** *125,* 10622–10631, https://doi.org/10.1021/acs.jpca.1c09359.
51. Pour Karim, S.; Ahmadi, R.; Yousefi, M.; Kalateh, K.; Zarei, G. Interaction of Graphene with Amoxicillin Antibiotic by in Silico Study. *Chemical Methodologies* **2022,** *6,* 861–871, https://doi.org/10.22034/chemm.2022.347571.1560.
52. Srivastava, A.K. Ionization of NO by superhalogens: DFT and QTAIM approaches. *Main Group Chemistry* **2021,** *20,* 33–40, https://doi.org/10.3233/mgc-210004.